

## Effect of atmospheric water vapor on modification of stable isotopes in near-surface snow on ice sheets

Michael S. Town,<sup>1</sup> Stephen G. Warren,<sup>1,2</sup> Von P. Walden,<sup>3</sup> and Edwin D. Waddington<sup>2</sup>

Received 22 January 2008; revised 3 July 2008; accepted 6 August 2008; published XX Month 2008.

[1] A Rayleigh fractionation model is developed to investigate postdepositional modification of stable isotopes of water in the near-surface snow of East Antarctica. The processes of forced ventilation, pore-space diffusion, and intra-ice-grain diffusion are parameterized through characteristic time constants. Routine meteorological observations, their derived products, and general glaciological conditions from the South Pole are used to simulate the  $\delta^{18}\text{O}$  of near-surface snow as it evolves in time. The sensitivity of  $\delta^{18}\text{O}$  of near-surface snow to wind speed, surface temperature, and accumulation rate is tested through model experiments. A steady wind of  $5\text{--}10\text{ m s}^{-1}$  results in annual mean  $\delta^{18}\text{O}$  enrichment of  $3\text{--}7\text{‰}$ . Enrichment of the heavy isotope occurs predominantly in buried winter snow layers during summer. However, in many simulations, there is a slight depletion of  $\delta^{18}\text{O}$  summer layers that occurs as atmospheric water vapor is deposited within the snow during winter. Postdepositional modification of water stable isotopes in near-surface snow also depends on the snow accumulation rate; high accumulation rates quickly advect snow layers away from the influence of the atmosphere, preventing significant modification. Low accumulation rates (e.g., at Vostok and Dome C) allow significant postdepositional modification because the near-surface snow is exposed to forced ventilation for several annual cycles. Postdepositional modification during the Last Glacial Maximum (LGM) at the Greenland Summit is estimated to be greater than the present-day postdepositional modification. Therefore the temperature difference for LGM may be larger than that previously inferred from the  $\delta^{18}\text{O}$  record. However, because of the compensating effects of lower temperatures and smaller accumulation during the LGM in Antarctica, the postdepositional enrichment in East Antarctica may be approximately the same for LGM as for the modern climate.

**Citation:** Town, M. S., S. G. Warren, V. P. Walden, and E. D. Waddington (2008), Effect of atmospheric water vapor on modification of stable isotopes in near-surface snow on ice sheets, *J. Geophys. Res.*, *113*, XXXXXX, doi:10.1029/2008JD009852.

### 1. Introduction

[2] Stable isotopes of water in polar snow and ice have long been regarded as proxies for local or regional temperature. This association was originally based on the relationship between mean annual temperature and the abundance of heavy isotopes of water found in water vapor and precipitation as functions of latitude [Dansgaard, 1964]. An important application of this relationship has been to reconstruct the temperatures of paleoclimates based on the stable-isotope content of the snow and ice found in polar regions [e.g., Lorius et al., 1979; Grootes et al., 1994; Petit et al., 1999; Johnsen et al., 2001; EPICA Members, 2004, and references therein]. Some recent efforts have focused on

reconstructing the recent past by drilling many short cores over a large region [e.g., Mayewski et al., 2005].

[3] While the results of these studies and their supporting atmospheric and glaciological investigations confirm the general conclusion that stable isotopes of water are related to local surface temperature, it is understood that the  $^{18}\text{O}$  content of polar snow is also affected by other variables [e.g., Jouzel et al., 1997, 2003]. Numerous studies in the past several decades have sought to refine our understanding of  $^{18}\text{O}$  in polar snow and ice in the hope of improving our understanding of paleoclimates and climates of the recent past [e.g., Jouzel et al., 1983; Whillans and Grootes, 1985; Cuffey and Steig, 1998; Johnsen et al., 2000; Helsen et al., 2005, 2006, 2007]. The discrepancy between the established spatially-based  $^{18}\text{O}$ -temperature ( $^{18}\text{O}$ -T) relationship [Dansgaard, 1964] and the newer temporally-based  $^{18}\text{O}$ -T relationship inferred from borehole temperature profiles [e.g., Cuffey et al., 1995] highlights the need for further insight into the factors influencing  $^{18}\text{O}$  in polar snow and ice.

[4] Isotopic concentrations in water are usually expressed by the deviation of the ratio of heavy to light isotopes from

<sup>1</sup>Department of Atmospheric Sciences, University of Washington, Seattle, Washington, USA.

<sup>2</sup>Department of Earth and Space Sciences, University of Washington, Seattle, Washington, USA.

<sup>3</sup>Department of Geography, University of Idaho, Moscow, Idaho, USA.

that of Standard Mean Ocean Water (SMOW). Both deuterium and  $^{18}\text{O}$  are commonly measured; however, in this paper we will consider only  $^{18}\text{O}$ . The concentration of  $^{18}\text{O}$  is expressed in “ $\delta$ ” notation in equation (1).

$$\delta^{18}\text{O} = \left[ \frac{\left( \frac{^{18}\text{O}}{^{16}\text{O}} \right)_{\text{sample}}}{\left( \frac{^{18}\text{O}}{^{16}\text{O}} \right)_{\text{SMOW}}} - 1 \right] \times 1000 \quad (1)$$

[5] Several factors affecting stable isotope concentrations are known; they can be separated into processes occurring before and after deposition. Before deposition, the  $\delta^{18}\text{O}$  of the water vapor and eventual condensate depend on the temperature and  $\delta^{18}\text{O}$  of the evaporative source, the humidity above the evaporative source, the air-parcel trajectory and desiccation history [Jouzel and Merlivat, 1984; Jouzel *et al.*, 2003; Helsen *et al.*, 2005, 2006, 2007], mixed-phase temperature thresholds, the relative abundance of liquid and ice [Ciais and Jouzel, 1994], and the final condensation temperature of the air parcel [Jouzel *et al.*, 1983]. Seasonality of precipitation can also cause biases in annual records [Cuffey and Steig, 1998; Krinner and Werner, 2003].

[6] Even if all the above factors are perfectly known, there are still several processes that may influence the isotopic content of snow after it has reached the surface and been advected downward by further accumulation. Mechanical processes such as mixing during blowing snow events, and seasonal scouring or spatial redistribution of snow can alter seasonal and annual records [Fisher *et al.*, 1983]. Diffusive transport of stable isotopes in the firn before close-off [Johnsen, 1977; Whillans and Grootes, 1985; Cuffey and Steig, 1998; Johnsen *et al.*, 2000] and after pore close-off also affects the seasonal and interannual  $\delta^{18}\text{O}$ .

[7] Given adequate accumulation rates, back-diffusion models can be used to reconstruct seasonal cycles of  $\delta^{18}\text{O}$ . Such reconstructions typically ignore the effect of surface conditions on recent snowfall and instead focus on the effects of vapor diffusion through pore spaces below approximately 1–2 m from the surface, away from the active influence of the atmosphere [e.g., Cuffey and Steig, 1998]. The effects of boundary-layer atmospheric water vapor on the isotopic content of near-surface snow are thought to fall off rapidly with depth [Waddington *et al.*, 2002]; it is therefore a good assumption that interstitial vapor diffusion is the dominant postdepositional process below the top meter or two of the snow surface. However, this does not mean that processes occurring just after deposition are not significant to the final isotopic content of snow. Redistribution of snow by wind is thought to explain a large fraction of the variance in the water stable isotope record at Vostok [Ekaykin *et al.*, 2002]. Epstein *et al.* [1965] proposed that depth-hoar formation may result in isotopic enrichment of snow layers at the South Pole. Neumann *et al.* [2005] suggested that wind pumping, pore-space diffusion, and intra-ice-grain diffusion may have a significant effect on isotopic composition of snow at Taylor Mouth (above the McMurdo Dry Valleys, Antarctica).

[8] In this work, we further explore postdepositional modification of cold (i.e., non-melting) Antarctic snow.

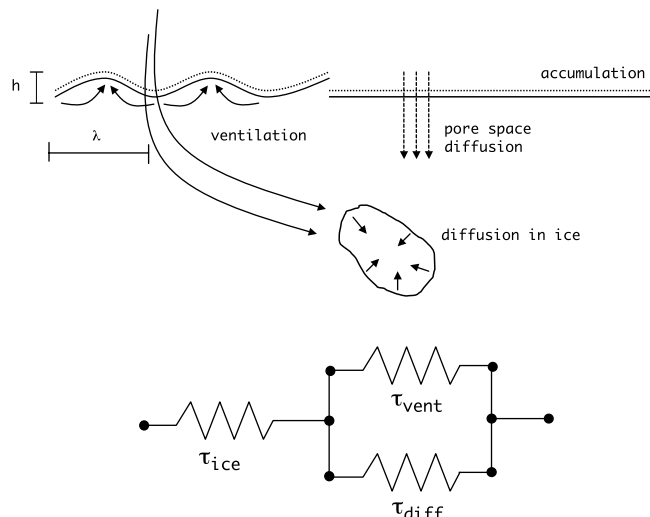


**Figure 1.** A depiction of the processes involved in the water stable isotope model. The processes of forced ventilation (i.e., wind pumping,  $\tau_{\text{vent}}$ ) and pore-space diffusion ( $\tau_{\text{diff}}$ ) act in parallel and in series with intra-ice-grain diffusion ( $\tau_{\text{ice}}$ ). Accumulation is added to the top volume of the model, with a  $\delta^{18}\text{O}$  signature related to the skin-surface temperature. At each time step, the top volume  $\delta^{18}\text{O}$  is a weighted average of the preexisting snow and the new snowfall. When the top volume becomes three times the original thickness of 5 mm, 1 cm of snow is advected downward. Below the top volume, only forced ventilation or pore-space diffusion will change the isotopic content of the snow.

Our goal is to understand the effects of weather and climate variability on the isotopic composition of near-surface snow. To achieve this end, we have developed a simple Rayleigh-fractionation model of postdepositional processes in cold snow based on time constants for diffusion of atmospheric water vapor, wind pumping, and solid-ice diffusion from Waddington *et al.* [2002]. To make the results as realistic as possible, we drive the model with meteorological data, and derived products, from the South Pole Station. With controlled model experiments in a range of different scenarios, we show that postdepositional modification of the near-surface snow may be significant under certain conditions, and that such modification affects the  $\delta^{18}\text{O}$  record stored in ice cores. We also explore the implications of our results for reconstructions of polar paleoclimatic temperatures.

## 2. Methods

[9] We simulate the change of water stable isotopes in near-surface snow using a Rayleigh fractionation model based on characteristic time constants developed by Waddington *et al.* [2002]. Rayleigh fractionation is an equilibrium process requiring the immediate removal of condensate after formation [Dansgaard, 1964]. Our model, depicted in Figure 1, includes ventilation, pore-space diffusion, and intra-ice-grain diffusion. The model advects or diffuses water vapor from the atmosphere to depth in the snow. After the water vapor is deposited in the snow, it

diffuses into the ice grain upon which it was deposited. This last step is necessary because if isotopically different water was deposited on, but not incorporated into, the snow grain, then the surface layer could easily sublimate, restoring the original isotopic content.

## 2.1. Stable Isotope Model

[10] The model described here includes the effects of surface temperature, subsurface temperature, accumulation rate, snow grain size, snow density, wind speed, and surface roughness on the of  $\delta^{18}\text{O}$  polar snow.

[11] As shown in Figure 1, the processes of diffusion and advection of water vapor into the snow occur in parallel. The time constant for diffusion of water vapor to depth in the snow is related to the temperature-dependent diffusion coefficient of water vapor in air ( $\kappa_{air}$ ) and the square of the depth ( $z$ ). We further multiply the quotient by  $n$  (see equation (2)), the number of times water vapor must be replaced through diffusion in a given pore space to completely replace the mass of the ice surrounding the pore space.

$$\tau_{diff}(z) = n \frac{z^2}{\kappa_{air}}, \quad (2)$$

where

$$n = \frac{(1 - \phi) \rho_{ice} P_{air}}{\phi \rho_{air} e_s(T)} \quad (3)$$

Here  $\phi$  is the porosity of the snow,  $\rho_{ice}$  and  $\rho_{air}$  are the densities of ice and air,  $P_{air}$  is the atmospheric pressure, and  $e_s(T)$  is the saturation vapor pressure at temperature  $T$ .

[12] Forced ventilation of snow was described by *Colbeck* [1989]. Using a sinusoidal surface topography of height  $h$  and length  $\lambda$ , pressure perturbations at the snow surface vary sinusoidally. They are also functions of the density of the air,  $\rho_{air}$ , and the square of the wind speed ( $U$ ). Equation (4) describes the amplitude of the pressure perturbations ( $p_o$ ) induced by the surface topography. The drag constant  $C$  is set to 3, which is optimized for drag along the dune axis and wind speeds measured at 10 m [*Cunningham and Waddington*, 1993].

$$p_o = C \rho_{air} U^2 \frac{h}{\lambda} \quad (4)$$

[13] By applying a sinusoidal pressure perturbation to the snow surface, *Waddington et al.* [1996] determined the amount of time for a single air exchange to occur at depth  $z$ . In equation (5),  $\tau_{vent}$  is this time multiplied by  $n$ , resulting in the number of air exchanges necessary to affect the isotopic content of the snow at depth  $z$ .

$$\tau_{vent}(z) = \frac{n \lambda^2 \phi \mu}{2\pi K p_o} e^{2\pi z/\lambda} \quad (5)$$

Here  $\mu$  is the atmospheric viscosity, and  $K$  is the permeability of the snow. We set  $\mu = 1.2 \times 10^{-5} \text{ m}^2 \text{ s}^{-1}$ , and  $K = 22 \times 10^{-10} \text{ m}^2$ .

[14] The time constant for diffusion of isotopes into the ice grain, equation (6), is proportional to the surface area of the ice grain, a geometrical factor  $G \approx 0.057$  [*Whillans and Grootes*, 1985], and a coefficient of diffusion for ice, taken as  $\kappa_{ice} = 5 \times 10^{-8} \text{ m}^2 \text{ a}^{-1}$  [*Waddington et al.*, 2002].

$$\tau_{ice}(z) = G \frac{[r(z)]^2}{\kappa_{ice}}, \quad (6)$$

where  $r$  is the snow grain radius.

[15] Two other processes were identified by *Waddington et al.* [1996, 2002] but determined to be insignificant relative to the three processes mentioned above. One process is forced ventilation of water vapor due to surface pressure variations from atmospheric turbulence. This process is slow and effectively short-circuited by both pore-space diffusion and forced ventilation due to surface roughness. The other process is diffusion of water across the thin, liquid-like layer on the surface of ice grains. This process is fast compared with both diffusion of water into the ice grain itself and the combined processes of pore-space diffusion and forced ventilation, and so it is not necessary to include it in the model.

[16] When all appropriate processes are combined, the final time constant is

$$\tau_{tot}(z) = \tau_{ice}(z) + \left( \frac{1}{\tau_{vent}(z)} + \frac{1}{\tau_{diff}(z)} \right)^{-1}. \quad (7)$$

[17] Molecular diffusion of atmospheric water vapor into the snow through pore spaces is really significant only in the top one or two centimeters of the snow on time scales relevant to natural accumulation rates on the Antarctic Plateau, or the high Greenland Plateau. Forced ventilation, on the other hand, will be significant in the top 10–40 cm depending on absolute temperatures, temperature gradients, wind speeds, and the surface roughness.

[18] When ice is formed through vapor deposition, there is a fractionation of water isotopes [*Dansgaard*, 1964] that we parameterize in the near-surface snow as a Rayleigh fractionation process, as in the work of *Neumann et al.* [2005]. In doing so, we assume that the air entering the snow is saturated with respect to ice, a value dictated by observed skin-surface temperatures. The assumption of ice saturation is valid over the Antarctic Plateau in all seasons; in fact, supersaturation with respect to ice is a common occurrence in the near-surface atmosphere [e.g., *Schwerdtfeger*, 1970; *Hogan*, 1975; *Town et al.*, 2005]. In the Rayleigh fractionation process simulated here, isotopically significant deposition of vapor occurs only when the atmosphere is warmer than the layer of snow to which the air is diffused or advected. In this model, the excess water vapor advected into the snow contributes to the isotopic composition in the following way:

$$\delta^{18}O_{ice}(z, t + \Delta t) = \delta^{18}O_{ice}(z, t) e^{-\Delta t/\tau_{tot}(z, t)} + \delta^{18}O_{vap}(0, t) \cdot \frac{1 - \beta(z, t)^{\alpha_{v-i}(T)}}{1 - \beta(z, t)} \left( 1 - e^{-\Delta t/\tau_{tot}(z, t)} \right). \quad (8)$$

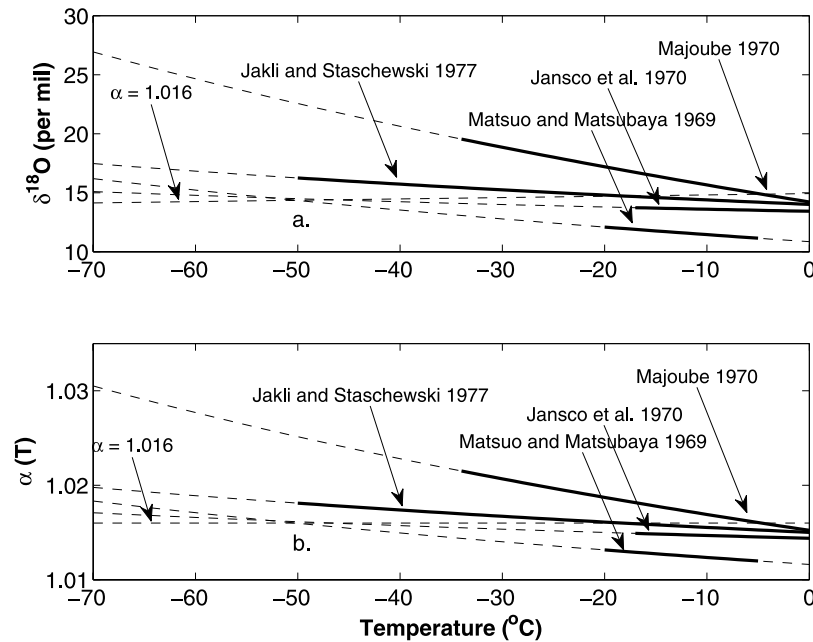


**Figure 2.** (a) The temperature dependence of the vapor-to-ice transition ( $\beta = 0.9$ ) plotted as the difference  $\delta^{18}\text{O}_{\text{ice}}$  relative to  $\delta^{18}\text{O}_{\text{vap}}$  using several different published relationships for  $\alpha(T)_{v-i}$  (equation (8)). (b) Temperature dependence of  $\alpha_{v-i}$  used in equation (8). The temperature dependencies are determined experimentally down to different temperatures (solid lines) but often extrapolated to lower temperatures (dashed lines). The temperature ranges of each formula are:  $-20^{\circ}\text{C}$  to  $-5^{\circ}\text{C}$  [Matsuo and Matsubaya, 1969],  $-17^{\circ}\text{C}$  to  $0^{\circ}\text{C}$  [Jansco et al., 1970],  $-33.4^{\circ}\text{C}$  to  $0^{\circ}\text{C}$  [Majoube, 1970], and  $-50^{\circ}\text{C}$  to  $0^{\circ}\text{C}$  [Jakli and Staschewski, 1977].

[19] Here the isotopic composition of ice at each time step depends on a weighted mean of the isotopic composition of the ice at the end of the previous time step and the isotopic composition of the vapor transported from just above the snow surface to depth and incorporated into the ice. Time steps are incremental ( $\Delta t = 1$  day). The ratio in the second term on the right-hand side of equation (8) represents Rayleigh fractionation, which converts the isotopic composition of the water vapor from the near-surface air to the fractionated isotopic composition after deposition at a given temperature. The variable  $\beta(z, t)$  is the ratio of the pore-space water-vapor content to the water-vapor content of the air parcel transported from the surface ( $z = 0$ ) to level  $z$  within the snow. The variable  $\beta(z, t)$  depends on  $z$  only in that the temperature of the snow, and therefore the pore-space saturation vapor pressure, changes with depth. We assume that the near-surface air and pore spaces are saturated with respect to ice, so that if a warmer air parcel from the surface is advected down to a colder level, then there will be deposition; i.e.,  $\beta(z, t)$  will be less than unity. The rate of water vapor advection to depth is prescribed by the time constants above.

[20] The variable  $\alpha_{v-i}(T)$  in equation (8) is the ratio of vapor pressure of  $\text{H}_2^{16}\text{O}$  to  $\text{H}_2^{18}\text{O}$ ; it is experimentally determined and temperature-dependent. The work of Majoube [1970] is the most commonly cited reference for  $\alpha_{v-i}(T)$  in polar stable-isotope literature, however, there are a number of other estimates of  $\alpha_{v-i}(T)$  [Matsuo and Matsubaya, 1969; Jansco et al., 1970; Jakli and Staschewski, 1977]. Figure 2 shows the effect of the different temperature dependencies on  $\alpha_{v-i}(T)$  and fractionation of during a vapor-to-ice transition of  $\beta = 0.9$ ; i.e., 10% of the

water vapor is deposited as ice. The parameter  $\alpha_{v-i}(T)$  has been experimentally determined to temperatures as low as  $-50^{\circ}\text{C}$  [Jakli and Staschewski, 1977], the mean annual temperature at the South Pole. However, not all  $\alpha_{v-i}(T)$  are determined to temperatures this low; e.g., Majoube [1970] only determined down to  $-33^{\circ}\text{C}$ , below which  $\alpha_{v-i}(T)$  values are extrapolated.

[21] Figure 2 shows differences among the available formulas in the amount of fractionation as a function of temperature. It is beyond the scope of this work to determine which  $\alpha_{v-i}(T)$  is the most accurate. The differences are largest at low temperatures for the scenario simulated here. Here, we use the relationship from the work of Majoube [1970] in accordance with prior literature, and characterize range of fractionation magnitudes for the different  $\alpha_{v-i}(T)$  relationships at South Pole temperatures. The sensitivity of our results to the range of available  $\alpha_{v-i}(T)$  is given below in the discussion of our model results. We show that the choice of the  $\alpha_{v-i}(T)$  has a negligible effect on our final answers, likely because the various  $\alpha_{v-i}(T)$  relationships are similar in the range of temperatures when vapor pressures are highest and postdepositional modification is largest.

[22] The snow density is set to be constant with depth at  $350 \text{ kg m}^{-3}$  in the top meter of snow, which is realistic for the South Pole [Figure 2 of Brandt and Warren, 1997]. The density profile does not change in the model as isotopic modification occurs. We are therefore assuming that sublimation equals deposition within the snow. If the density of the snow were to increase, the number of required air exchanges would increase while permeability decreases, lowering the rate of  $\delta^{18}\text{O}$  modification for a given climate regime. We have found that the model is not very sensitive

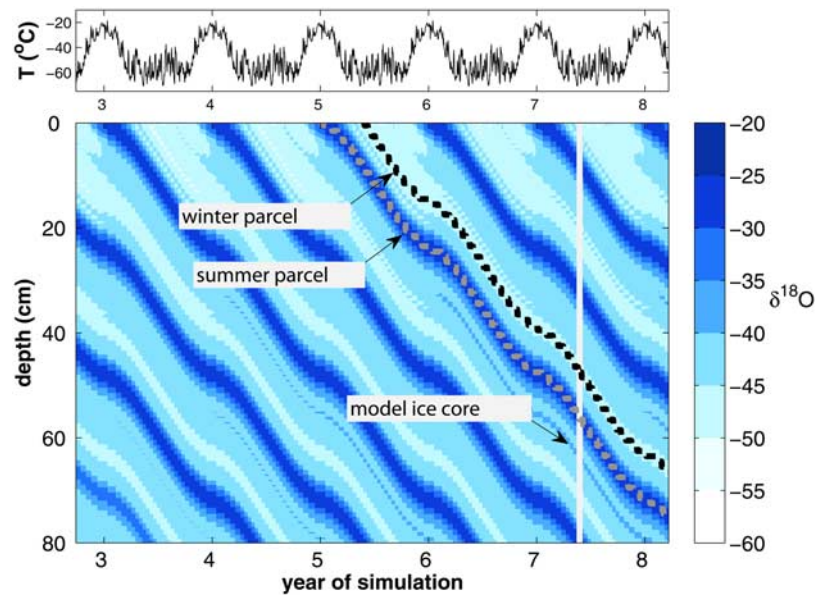


**Figure 3.** Sample output from the stable-isotope model. (top) Mean daily temperatures from the South Pole for 1996 repeated 9 times to provide an upper boundary condition. (bottom)  $\delta^{18}\text{O}$  of the snow. Snow falls with a  $\delta^{18}\text{O}$  value related to the skin-surface temperature, wind speeds are set to  $5 \text{ m s}^{-1}$ , the annual accumulation rate is  $24 \text{ cm a}^{-1}$ , and the surface roughness is parameterized as  $h = 0.2 \text{ m}$  and  $\lambda = 1 \text{ m}$  (where  $h$  and  $\lambda$  are defined in Figure 1). In this case, the monthly accumulation rate in winter is three times that of summer, so contours of constant  $\delta^{18}\text{O}$  are wavy. The dashed lines are snow parcel trajectories, the contents of which are shown in Figure 4. Subsequent results are presented as model “ice cores” from early winter of the seventh year, after the model has lost all memory of its initial conditions. The model output shown here is for fractionation independent of temperature ( $\alpha_{v-i} = 1.01$ ). Tick marks indicate 1 January.

to snow-grain radius. Throughout the model, the radius is set to  $100 \mu\text{m}$ , a value representative of the top meter of snow at the South Pole [Grenfell et al., 1994].

[23] We also assume that isotopic fractionation does not occur during sublimation [e.g., Friedman et al., 1991; Neumann et al., 2005]. Although recent experimental evidence suggests that isotopic fractionation may occur during sublimation of snow at higher temperatures [Stichler et al., 2001; Neumann et al., 2008], the temperatures that we simulate here inhibit rapid isotopic homogenization of ice grains and suppress the thickness of the quasi-liquid layer on ice grains, both of which are thought to be important in fractionation during sublimation.

[24] The model spans 1 m in total depth and is divided into layers of 1 cm each, with a half-layer of 5 mm at the upper and lower boundaries. The  $\delta^{18}\text{O}$  of the accumulation is parameterized by equation (9):

$$\delta^{18}\text{O}_{\text{new snow}} = 0.75 T_{\text{skin}} - 15, \quad (9)$$

where  $T_{\text{skin}}$  is the temperature of the top millimeter of the snow in Celsius, as derived from upwelling longwave radiation measured at the South Pole. This temperature is also used as the temperature of the top 5 mm of the snow, as in the work of Town et al. [2008]. The  $\delta^{18}\text{O}$  of the surface water vapor advected into the snow is the Rayleigh-fractionation vapor equivalent of the new snow  $\delta^{18}\text{O}$  from (9).

[25] Equation (9) is approximately the  $\delta^{18}\text{O}$ -temperature relationship derived from spatial studies across Antarctica

[Dansgaard et al., 1973; Lorius et al., 1979]. Other  $\delta^{18}\text{O}$ -T relationships specific to the South Pole are available [Aldaz and Deutsch, 1967; Jouzel et al., 1983]. They have a greater sensitivity of  $\delta^{18}\text{O}$  to temperature ( $1.4\text{--}1.6\text{‰ K}^{-1}$ ), which would exaggerate the  $\delta^{18}\text{O}$  seasonal cycle in surface water vapor and new snow, and thereby enhance the postdepositional effects modeled here.

[26] Accumulation with  $\delta^{18}\text{O}$  from (9) is added to the top level of the model at each time step until the top level is 3 times (1.5 cm) its original depth. The model accumulation process averages the isotopic content of the top level with the isotopic content of the new snowfall. Once the top level has grown to 1.5 cm, 1 cm of it is advected downward to the adjacent lower level; all the layers of the model move down 1 cm, and 1 cm of the model is removed from the lower boundary. This parameterization of accumulation is realistic in that the surface snow does not stay perfectly, chronologically stratified after deposition because of mechanical mixing by wind drifting until sufficient accumulation buries the surface snow.

[27] Figure 3 shows model output when a measured annual cycle of daily surface temperature at the South Pole (top) is repeated many times. Daily wind speeds (not shown) are set to be constant at  $5 \text{ m s}^{-1}$  for the entire simulation. Accumulation of snow is set to be  $24 \text{ cm a}^{-1}$  ( $8.4 \text{ cm a}^{-1}$  liquid water equivalent, lwe, Mosley-Thompson et al. [1999]), but varies seasonally (3 times greater in winter than in summer; Bromwich and Parish [1998]). The color contours of Figure 3 depict the  $\delta^{18}\text{O}$  of the snow as it is

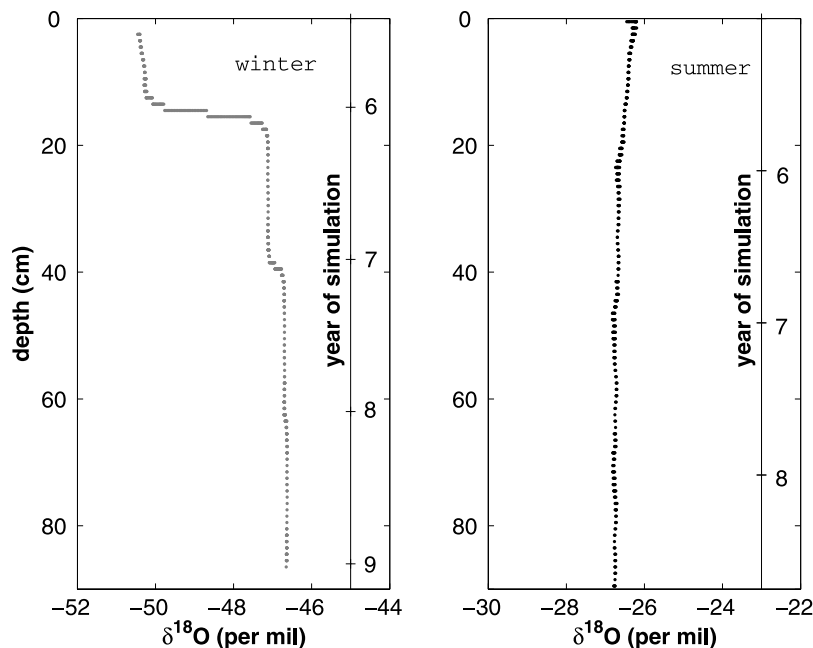


**Figure 4.** Isotopic content of snow parcels following the trajectories shown in Figure 3. Yearly tick marks on second  $y$  axis indicate 1 January.

advected downward. The model is initialized with a constant  $\delta^{18}\text{O}$ , and time steps continue until the initial snow leaves the model domain. Results presented in the following sections are primarily model “ice cores” from simulations similar to this one in which the boundary conditions are varied. The “ice cores” are all drilled during early winter, day 2700 of the simulation, unless otherwise noted.

[28] Qualitative interpretation of Figure 3 here will aid understanding of the quantitative results presented in later sections. In the absence of wind, the seasonal cycle of  $\delta^{18}\text{O}$  advected into the model snowpack will depend primarily on the surface temperature and the seasonal accumulation rate; diffusion of atmospheric water vapor into the snow will still occur, but its overall effect on  $\delta^{18}\text{O}$  has been determined to be small here. In Figure 3, the accumulation rate varies with season, so the  $\delta^{18}\text{O}$  contours are wavy, with downward advection (accumulation) slowing during summer and speeding up during winter. Surface winds over the undulating surface ( $h = 0.2$  m,  $\lambda = 1$  m; see Figure 1) forces water vapor into and out of the snow. Snow depleted in  $^{18}\text{O}$ , which fell during the winter, is enriched during the following summer as the temperature contrast between the surface and deeper snow increases, and water-vapor-laden air is forced into the snow by surface winds over the surface topography. Because of its proximity to the surface in summer, the late-winter snow experiences greater enrichment than early-winter snow. The winter snow is further enriched during later summers, but the rate of enrichment is attenuated because the winter layers are farther from the surface in subsequent years.

[29] The dashed lines in Figure 3 represent snow-parcel histories for snow deposited during winter and summer. The  $\delta^{18}\text{O}$  content of two snow parcels and timing of postdepositional modification are shown in Figure 4. The winter snow parcel shown here experiences most of its enrichment of  $^{18}\text{O}$  in the first summer following deposition (beginning

of simulation year 6 in Figure 4). Further enrichment of winter snow occurs in the third summer after deposition (beginning of simulation year 8 in Figure 4), but it is small. The summer snow parcel experiences a small, steady depletion of  $^{18}\text{O}$  during the first winter after deposition (simulation year 5 in Figure 4), but then essentially no change after that.

[30] These qualitative results suggest that the influence of subsequent summers on the  $\delta^{18}\text{O}$  of winter snow will depend on the magnitude of the seasonal cycles in temperature and accumulation rate, and on absolute temperatures, accumulation rates, wind speeds, and surface morphology. A large accumulation rate will advect the surface snow away from the surface quickly, reducing the effect of forced ventilation on the  $\delta^{18}\text{O}$  values. This sketch of postdepositional modification processes in near-surface snow will be further refined in sections 3 and 4.

[31] We tested the sensitivity of our results to diffusion of water stable isotopes across isotopic gradients, as described by *Johnsen et al.* [2000]; it is not significant for the time scales presented here (on the order of a few tenths of a ‰ over several years), and was left out of the quantitative analysis presented below.

[32] The model described here uses simple parameterizations of complex physics. More complex simulations are possible; however, given the uncertainties that may be introduced by assumptions inherent to the simulation such as evolving surface morphology and the isotopic content of water vapor, this level of model complexity is appropriate for our goals.

## 2.2. Input Data

[33] The input data for this model come primarily from routine meteorological observations made at the South Pole Station and from model output from a finite-volume thermal diffusion model of the near-surface snow, described by *Town et al.* [2008]. The routine observations are made by

the National Oceanic and Atmospheric Administration (NOAA) Earth and Space Research Laboratory - Global Monitoring Division (ESRL-GMD). The daily or seasonal skin-surface temperatures used here are derived from upwelling longwave-radiation fluxes from 1994 to 2003 with time resolution 1–3 minutes. The 10-m wind speeds were measured at 1-minute intervals and averaged to daily or longer time periods.

[34] The top of Figure 3 depicts a repeated annual cycle of mean daily temperatures for the South Pole from 1996. This time series is used as an upper boundary condition in some of the simulations below. Other simulations use an average seasonal cycle of surface temperatures for 1995–2003. This span of years is chosen based on the availability of modeled subsurface temperatures, discussed below.

[35] The mean annual 2-m air temperature of the South Pole is approximately  $-50^{\circ}\text{C}$ , with a mean summer-to-winter temperature difference of approximately 30 K. Daily temperature variability is greater during the long, *coreless* winter (April–September, *Schwerdtfeger* [1970]) than during the short summer (December–January). The year 1996 exhibited a “mid-winter warming”, a phenomenon previously noticed in  $\delta^{18}\text{O}$  records in Antarctica [e.g., *Steig et al.*, 2005], which makes 1996 an interesting year to simulate. Isotopically, the mid-winter warming is an enrichment pulse in the coreless-winter signal. Synoptically, the mid-winter warming is a particularly stormy interval associated with enough accumulation to leave an isotopic signal in the snow record. Mid-winter warmings are also associated with higher winds, and therefore more mechanical mixing of the surface snow, as well as increased near-surface snow modification.

[36] The 10-m wind speeds at the South Pole can vary from  $1\text{--}2\text{ m s}^{-1}$  to  $15\text{--}20\text{ m s}^{-1}$ . The mean annual wind speed at the South Pole is approximately  $5\text{ m s}^{-1}$ , with a small seasonal cycle ranging from  $4\text{ m s}^{-1}$  in summer to  $6\text{ m s}^{-1}$  in winter.

[37] The annual accumulation rate for the South Pole is taken from the work of *Mosley-Thompson et al.* [1999], approximately  $8.4\text{ cm a}^{-1}$  lwe. Evidence suggests that much of the accumulation over the Antarctic Plateau occurs during winter [*Bromwich and Parish*, 1998; *Mosley-Thompson et al.*, 1999], and that summer may even be a time of net ablation [*Mosley-Thompson et al.*, 1999]. We either simulate accumulation as constant throughout the year or set the monthly accumulation rate during winter to be three times that of summer, with linear transitions during spring and autumn in the seasonal simulations (as inferred from Figure 3). In reality, accumulation at the South Pole comes largely in two forms: as snow grains that form in clouds aloft (as a result of advection of moisture from the coast), or as clear-sky precipitation (“diamond dust”) that forms throughout the steep temperature inversion layer during calm periods on the Antarctic Plateau. Because of the low temperatures over the South Pole, we do not expect frost deposition to be a significant source of mass. The combination from falling snow grains and diamond dust makes accumulation at the South Pole approximately continuous, though variable in rate. The relative contribution of diamond dust to total accumulation increases as one proceeds to the highest regions of the Antarctic Plateau because high elevations inhibit the direct influences of coastal synoptic activity. The contribution of diamond dust to total accumulation on the East Antarctic Plateau may be as high as 50–80% in places

[*Kuhn et al.*, 1975; *Ekaykin et al.*, 2004; *Fujita and Abe*, 2006].

[38] The subsurface temperatures driving the model are taken from the work of *Town et al.* [2008]. The calculated temperatures have the same temporal resolution as the upwelling longwave data and are averaged to daily or longer times, depending on the scenario. Saturation with respect to ice is assumed within the snow pore-spaces, using snow temperatures from the work of *Town et al.* [2008].

[39] Snow temperatures at the South Pole are an integrated response of the snow to the heat content from the previous season and the large day-to-day variations in atmospheric temperature. The thermal conductivity of the snow produces temporal lags in temperature with depth so that a layer of snow may be heated or cooled from below as well as from above. Atmospheric temperature variability is the main driver of changes in near-surface snow temperatures, so the largest variations in snow temperature occur near the surface. Near-surface temperature gradients in the snow vary on synoptic time scales, and may even change sign several times during a month depending on the synoptic conditions. The standard deviations of 9-minute temperatures in the top 10 cm of the snow at the South Pole are 3 K during summer and 6 K during winter; computed heating rates exceeding  $10\text{ K day}^{-1}$  occur throughout the year [*Town et al.*, 2008]. Such rapid changes of snow temperatures, coupled with the thermal lag inherent in the snow, can result in significant snow-air temperature contrast. This temperature contrast allows wind pumping to exchange air masses with different vapor pressures, resulting in postdepositional modification of water stable isotopes in the near-surface snow.

### 3. Modification of $\delta^{18}\text{O}$ due to Temperature, Wind-Speed, and Accumulation Variability

[40] In this section, we present results of modification of water stable isotopes by examining model “ice cores,” as illustrated in Figure 3. Smooth or variable seasonal cycles of temperature and wind speeds are first applied to the upper boundary of the model. We then investigate the effect of seasonality of accumulation on modification of  $\delta^{18}\text{O}$ , as well as the sensitivity of the model to different mean annual accumulation rates.

#### 3.1. Variable Temperatures and Wind Speeds

[41] To investigate the effect of temperature and wind-speed variability on the  $\delta^{18}\text{O}$  of the snow, we first simulate two cases that experience no postdepositional modification. The first case, the gray curve in Figure 5a, incorporates the climatology of monthly mean surface and subsurface temperatures averaged for 1995–2003. Snow accumulates at a constant rate of  $24\text{ cm a}^{-1}$  of snow ( $8.4\text{ cm a}^{-1}$  lwe). The second case, the gray curve in Figure 5c, incorporates mean daily surface and subsurface temperatures for the year 1996 with the same constant accumulation rate,  $24\text{ cm a}^{-1}$ . We keep the snow grain radius and snow density constant with depth at  $100\text{ }\mu\text{m}$  and  $350\text{ kg m}^{-3}$ , respectively.

[42] These baseline cases illustrate some important features. The  $\delta^{18}\text{O}$  records also show a depleted, coreless winter punctuated by short, enriched summers. The simulation in Figure 5c uses the temperature time series shown in

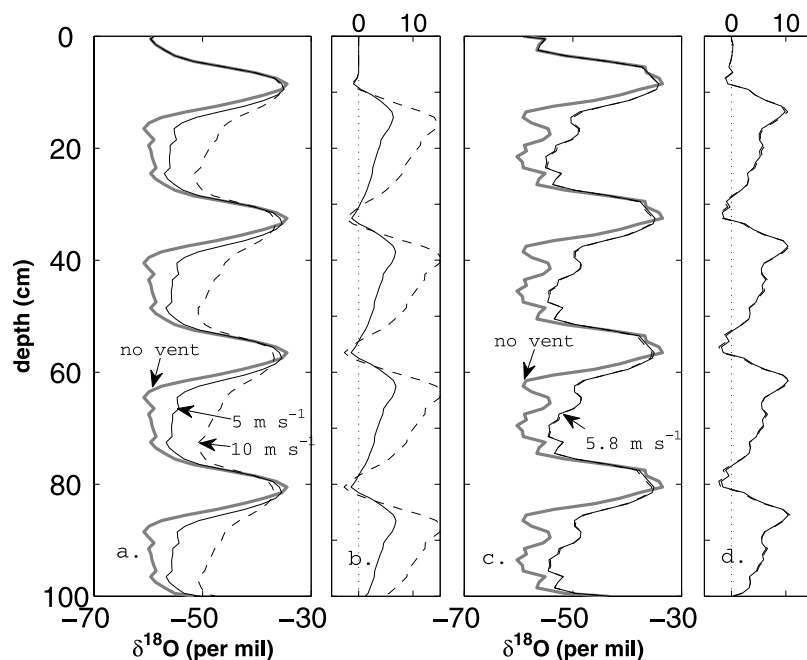


**Figure 5.** Model ice cores illustrating the influence of temperature variability and wind-speed variability on postdepositional modification of stable isotopes in snow. (a) Three simulations based on mean temperatures for the South Pole for 1995–2003. The cases are no wind (solid gray) and constant surface wind of  $5 \text{ m s}^{-1}$  (solid black) and  $10 \text{ m s}^{-1}$  (dashed black). (b) The residual of the  $5 \text{ m s}^{-1}$  case minus the windless case (solid black) and  $10 \text{ m s}^{-1}$  case minus the windless case (dashed black). (c) Three simulations based on mean daily temperatures for the South Pole in 1996. The cases are no wind (solid gray), constant mean annual wind speed during 1996 (solid black), and mean daily wind speeds (dashed black). (d) The residual of the mean annual case minus the windless case (solid black) and similarly for the mean daily case (dashed black); the lines are almost indistinguishable.

the top of Figure 3; however, the resulting  $\delta^{18}\text{O}$  time series is much smoother than the temperature time series because of the averaging that occurs in the parameterization of accumulation in the top volume of the model (i.e., the 1 cm sampling resolution of the model).

[43] The simulations shown in Figure 5a include surface winds set at constant values of  $5 \text{ m s}^{-1}$  (solid black) and  $10 \text{ m s}^{-1}$  (dashed black). The resulting  $\delta^{18}\text{O}$  profiles differ dramatically from the baseline case with no surface winds. The mean annual snow is enriched by  $3.1\text{‰}$  for winds of  $5 \text{ m s}^{-1}$  and  $7.4\text{‰}$  for winds of  $10 \text{ m s}^{-1}$  (Figure 5b; Table 1). The  $10 \text{ m s}^{-1}$  case shows more than twice as much  $^{18}\text{O}$  enrichment as the  $5 \text{ m s}^{-1}$  case because forced ventilation of the snow depends on the square of the wind speed (equations (4) and (5)). The reason net enrichment is not four times as great when wind speed is doubled is discussed at the end of the section.

[44] The timing of the winter  $^{18}\text{O}$  enrichment is not easy to infer from these plots. In Figure 3, one can see that the winter snow is enriched during following summers. For typical wind speeds and surface roughness at the South Pole, water vapor during summer has the potential to affect two previous winters; we will show in the following subsection that this is also a function of the accumulation rate. Another feature of these simulations with constant annual accumulation rates is that the enrichment of late-winter snow during the following summer effectively broadens the enriched summer  $\delta^{18}\text{O}$  peak by a few weeks.

[45] There is a slight depletion of  $^{18}\text{O}$  in the summer maxima of the model ice core, by about  $1\text{‰}$  and  $2\text{‰}$  for  $5$  and  $10 \text{ m s}^{-1}$  winds, respectively. However, when averaged over the summer, the depletion is partly offset by the enrichment of the early-summer snow (see Table 1). As mentioned earlier, “depletion” does not occur from sublimation but is instead a result of deposition of isotopically depleted water vapor into a relatively enriched snow layer. With constant wind speeds, this depletion occurs episodically during winter and consistently during spring when atmospheric temperatures are higher than the buried summer snow temperatures but lower than the summer atmospheric temperatures responsible for the initial  $^{18}\text{O}$  of the snow layer. There are two reasons for the small magnitude of  $\delta^{18}\text{O}$  depletion in a summer snow layer. The low vapor content of the atmosphere during winter and spring inhibit large mass fluxes of water vapor, and the thickness of the winter snow layer between the surface and the previous summer snow layer impedes the influence of the atmosphere on the summer snow layer during winter and spring.

[46] Figure 5c shows simulations with a constant mean annual wind speed and the daily mean wind speed during 1996 coincident with the daily mean temperatures. The differences between the variable- and constant-wind-speed cases are small; they are barely visible in Figure 5d. The daily-varying-wind-speed and constant-wind-speed simulations show enrichment during winter. The difference in mean winter enrichment between the two simulations is on the order of  $0.1\text{--}0.2\text{‰}$  (Figure 5d). The difference in

**Table 1.** Postdepositional Modification in Near-Surface Polar Snow After the Snow Has Been Advected Below the Influence of the Atmosphere<sup>a</sup>

Row	$T_{\text{ann}}$ (°C)	acc (cm a <sup>-1</sup> )	ws (m s <sup>-1</sup> )	$\Delta \delta^{18}\text{O}_{\text{ann}}$ (‰)	$\Delta \delta^{18}\text{O}_{\text{win}}$ (‰)	$\Delta \delta^{18}\text{O}_{\text{sum}}$ (‰)	Figure
1	-50	24 (8.4 lwe)	5	3.1	4.0	-0.5 (-1.0)	5a, 5b
2	-50	24 (8.4 lwe)	10	7.4	11.0	-1.4 (-2.3)	5a, 5b
3	-47	8 (2.8 lwe)	5	8.6	13.0	-1.1 (-1.1)	7a
4	-47	24 (8.4 lwe)	5	3.6	4.1	-0.1 (-1.2)	7b
5	-47	72 (25.2 lwe)	5	0.9	0.8	0.0 (-0.7)	7c
6	-57	12 (4.2 lwe)	5	3.6	4.3	-0.2 (-0.2)	not shown
7	-57	24 (8.4 lwe)	5	1.5	1.6	0.2 (-0.4)	not shown
8	-47	18 (6.3 lwe)	5	5.1	6.6	-1.1 (-0.6)	8a, 8b
9	-47	36 (12.6 lwe)	5	2.3	2.6	-0.1 (-0.9)	not shown
10	-27	72 (25.2 lwe)	5	3.8	4.7	-0.9 (-2.8)	8a, 8b

<sup>a</sup>The left columns are the boundary conditions. The center columns show the enrichment of the annual mean, the winter mean, and the summer mean caused by forced ventilation. The symbol  $\Delta \delta^{18}\text{O}$  represents the difference between the wind and no-wind cases. The summer results in parentheses are the differences in *peak* summer values of  $\delta^{18}\text{O}$  due to ventilation, even if the peaks are shifted slightly in depth due to postdepositional modification. The rightmost column lists the figure in which these results are presented graphically. Winter is defined as April–September, summer is December–January. Rows 1 and 2 illustrate the effect of wind speed (ws). Rows 3–5 illustrate the effect of accumulation rate (acc). Rows 6–10 illustrate the effects of accumulation rate and temperature in different combinations designed to represent Antarctica and Greenland at present and at the LGM. Rows 1 and 2 are based on a 9-year mean of temperatures; all other rows are based on daily temperatures from a repeated annual cycle for a single year. Accumulation rates are given both in actual snow height ( $\rho_{\text{snow}} = 350 \text{ kg m}^{-3}$ ) and in liquid-water equivalent (lwe).

mean winter enrichment between using daily temperatures and monthly mean temperatures to simulate enrichment (not shown) is also on the order of a few tenths of a ‰.

[47] It is somewhat surprising that ventilation forced with daily wind speeds would not change the winter enrichment very much relative to ventilation forced with a constant wind speed of the same annual mean. Forced ventilation depends on the square of the wind speed (equation (4)), and so we might expect modification to increase as wind-speed variability increases, but leave the annual mean unchanged.

[48] There are two significant reasons why variable wind speeds do not have a net enriching effect on near-surface snow. First, at the South Pole the mean wind speed was  $5.8 \text{ m s}^{-1}$  during 1996, a wind speed very similar to the root mean square wind speed for that year ( $6.1 \text{ m s}^{-1}$ ), and representative of other years. So, we expect a maximum of approximately 10% enrichment because of this difference, but the modeled enrichment is even less than this; note that this wind-speed distribution is specific to the South Pole and may not occur at other ice-core sites.

[49] Second, any winter layer that experiences enrichment during a summer will also experience a “depletion” during a subsequent winter. Wintertime depletion can then counteract some summertime postdepositional enrichment. For example, large enrichment of a new winter snow layer can occur during the first summer after deposition. During subsequent winters, high wind speeds can lead to a large wintertime depletion of the same layer, because the enriched winter layer now has a  $\delta^{18}\text{O}$  content more similar to summertime water vapor than wintertime water vapor. At higher wind speeds ( $\approx 15 \text{ m s}^{-1}$ ), steady-wind-speed cases exhibit slightly greater winter layer enrichment than variable-wind-speed cases (not shown). The enhanced postdepositional modification under variable winds, as opposed to a steady-wind case of the same mean value wind speed, thus acts in both the enrichment and depletion directions such that the two effects partly offset each other. This is an additional reason why doubling the constant wind speed in our model does not quadruple the isotopic enrichment.

[50] Finally, in testing the sensitivity of our results to the choice of fractionation coefficients, we applied the range of available  $\alpha_{v-f}(T)$  given in section 2.1 to the scenarios shown in Figures 5a and 5b (results not shown). The mean annual enrichment ranges only 0.2‰ when winds are set to  $5 \text{ m s}^{-1}$ ; the range increases to approximately 0.4‰ when winds are increased to  $10 \text{ m s}^{-1}$ . The largest enrichment effect is seen when using the relationship for  $\alpha_{v-f}(T)$  of *Matsuo and Matsubaya* [1969], the smallest when using that of *Majoube* [1970]. The reason for the insensitivity of our results to the different formulas for  $\alpha_{v-f}(T)$  is probably that all the  $\alpha_{v-f}(T)$  formulas are close to each other at warmer temperatures, where most of the postdepositional processing occurs in our model.

### 3.2. Variable Accumulation Rates

[51] In this section we examine the effects of seasonally and annually varying accumulation rates. The effects of different annual accumulation rates are relevant not only for forced ventilation, but also for averaging that occurs in the top volume of the model. We use mean daily temperatures as model boundary conditions in these simulations so that the effects of the top-volume averaging (i.e., mechanical mixing) are more obvious.

[52] It is understood that a seasonally varying accumulation rate will bias the mean annual  $\delta^{18}\text{O}$  of an ice core [*Cuffey and Steig*, 1998; *Krinner and Werner*, 2003]. The effect of a seasonally variable accumulation rate in our model is shown in Figure 6. A steady rate throughout the year (the gray curve) is compared to a seasonal cycle in which the winter rate is three times the summer rate (the thin, solid curve), but keeping the same mean annual accumulation ( $24 \text{ cm a}^{-1}$ ). The residual between the two curves is plotted in Figure 6b.

[53] These simulations show that such a seasonality in precipitation induces an overall negative bias in the mean annual  $\delta^{18}\text{O}$  of approximately 2.6‰ relative to the mean annual  $\delta^{18}\text{O}$  if accumulation were constant throughout the year. The largest negative bias occurs during the spring as the accumulation rate decreases to summer levels; the

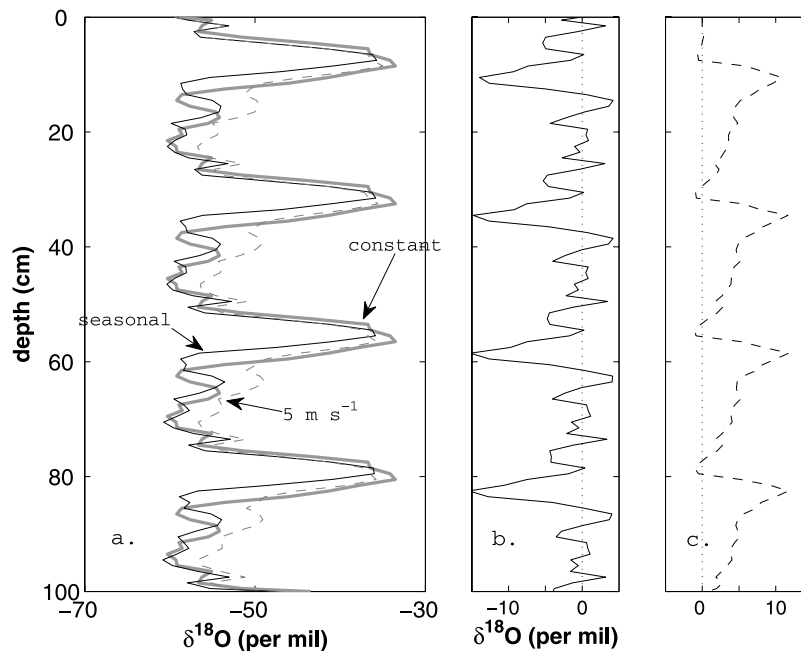


**Figure 6.** Variations in  $\delta^{18}\text{O}$  due to a seasonally variable accumulation rate. (a) A constant accumulation rate with no wind (solid gray), a seasonal accumulation rate with no wind (solid black), and a seasonal accumulation rate with a constant wind speed of  $5 \text{ m s}^{-1}$  (dashed black). (b) The windless seasonal-accumulation-rate case minus the windless constant-accumulation-rate case. (c) The  $5 \text{ m s}^{-1}$  seasonal-accumulation-rate case minus the windless seasonal-accumulation-rate case. The monthly accumulation rate in winter is three times that of summer. The total accumulation rate is kept at  $24 \text{ cm a}^{-1}$  ( $8.4 \text{ cm a}^{-1}$ ) for all cases. The boundary conditions are mean daily temperatures and vapor pressures for the South Pole from 1996.

timing of this difference is a result particular to the date of the model ice core’s “extraction”. The summer  $\delta^{18}\text{O}$  peak in the seasonal case is biased low relative to the constant-accumulation-rate case because of the top-volume averaging. Less snow falls during the summer in the seasonal-accumulation-rate case, resulting in averaging of more  $\delta^{18}\text{O}$  values corresponding to lower temperatures, than in the constant-accumulation-rate case.

[54] Adding a constant wind speed of  $5 \text{ m s}^{-1}$  to the seasonal-accumulation-rate case (dashed line) shows the same pattern of  $^{18}\text{O}$  enrichment (Figure 6c) as in the constant-accumulation-rate case (Figure 5d). One unique result when there is more accumulation during winter in the seasonal-accumulation-rate case; more winter snow is subjected to relatively enriched atmospheric water vapor than in the constant-accumulation-rate case. Another result is that the maximum  $^{18}\text{O}$  enrichment occurs not during late winter but rather during spring. In spring, temperatures are rising but the decrease in accumulation rate coupled with the top-volume averaging prevents new snow from reflecting the increase in temperature as strongly as in the constant-accumulation-rate case.

[55] Accumulation rate was found to be inversely proportional to the amount of postdepositional modification at Taylor Mouth, Antarctica [Neumann *et al.*, 2005]. We investigate this concept in Figure 7. Here, the annual accumulation is varied, but the accumulation rate is kept constant throughout the year. The three snow accumulation rates depicted are  $8$ ,  $24$ , and  $72 \text{ cm a}^{-1}$  ( $2.8$ ,  $8.4$ ,  $25.2 \text{ cm a}^{-1}$  lwe). These different accumulation rates approximately

represent three locations where deep ice cores have been drilled: Dome Concordia, South Pole, and Summit, Greenland. Of course, the temperature time series driving the model are from the South Pole, so the results cannot extend past this controlled analogy desired to isolate the effect of accumulation rate on postdepositional modification.

[56] The gray curves in Figure 7 show that the annual cycle is attenuated as the mean annual accumulation rate decreases; this is again due to top-volume averaging in the surface snow. A constant wind speed of  $5 \text{ m s}^{-1}$  has a large effect on the low-accumulation-rate simulation, but much less in the high-accumulation-rate simulation (Figure 7c). In the high-accumulation-rate simulations, there is slight  $^{18}\text{O}$  depletion during summer, and some enrichment in spring and late winter. The autumn and early winter  $\delta^{18}\text{O}$  levels are essentially unmodified by forced ventilation. The  $24 \text{ cm a}^{-1}$  case was discussed above.

[57] The low-accumulation-rate case (Figure 7a) shows enrichment, year after year, until approximately  $40 \text{ cm}$  in depth. The summer peaks are broadened, and the peak values are initially enriched by  $1\text{--}2\%$ . The enrichment occurs because the summer atmospheric water vapor deposited within the snow has greater  $\delta^{18}\text{O}$  than recorded in the  $1 \text{ cm}$  accumulation layers because of sampling resolution. The peak summer enrichment decreases slightly with depth as the influence of forced ventilation during winter compensates for the initial  $\delta^{18}\text{O}$  postdepositional enrichment during summer. The recorded coreless winter, initially short because of top-volume averaging, is significantly enriched because of forced ventilation.

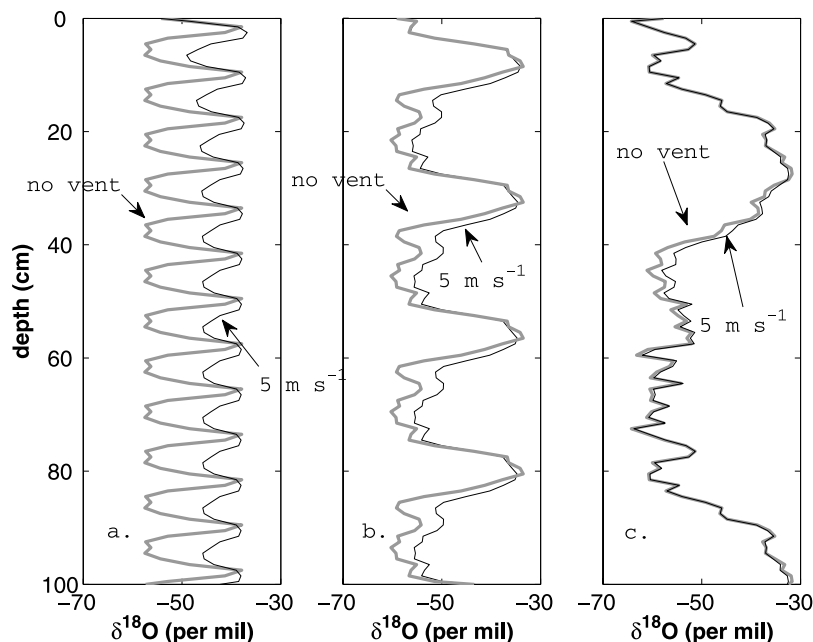


**Figure 7.** The effect of variable annual accumulation rates on postdepositional modification of  $\delta^{18}\text{O}$ . The solid gray lines indicate windless cases, and the solid black lines indicate the  $5\text{ m s}^{-1}$  cases. Accumulation rates in  $\text{cm a}^{-1}$  are 8, 24, and 72 in Figures 7a, 7b, and 7c, respectively (liquid-water equivalents 2.8, 8.4, and 25.2). Figure 7a is taken from the 13th year of the simulation with the low accumulation rate. The boundary conditions are mean daily temperatures for the South Pole from 1996.

[58] The low-accumulation-rate case experiences much more enrichment than the other two cases because the near-surface snow experiences the effects of forced ventilation during several summers. Low-accumulation-rate sites on the Antarctic Plateau may experience lower wind speeds than those at the South Pole, so the enrichment in Figure 7a is probably exaggerated. However, in cases where low-accumulation-rates are due partly to wind scouring, as may occur in katabatic wind zones, these wind speeds may be more realistic.

## 4. Discussion

[59] The results presented here may have significant implications for the interpretation of isotopic records of paleoclimates. We also present several ways to improve this model.

### 4.1. Interpretation of the Seasonal Cycle

[60] It is clear from Figures 5, 6, and 7 that forced ventilation of the snow enriches the winter  $\delta^{18}\text{O}$  levels, often slightly depleting summer  $\delta^{18}\text{O}$  levels, but overall adding a positive bias to the mean annual  $\delta^{18}\text{O}$  signal. Enrichment of winter layers was also found by *Neumann and Waddington* [2004] in a more complex 2-dimensional model with simpler boundary conditions. Forced ventilation also attenuates the amplitude of the seasonal cycle in  $\delta^{18}\text{O}$ . If one were to use the model ice-core data after postdepositional modification to develop a relationship between  $\delta^{18}\text{O}$  and temperature, then the seasonal sensitivity of  $\delta^{18}\text{O}$  to temperature would seem to change from the original model slope of 0.75 (equation (9)) to between 0.50 and  $0.33\% \text{ K}^{-1}$  for mean annual wind speeds between 5 and  $10\text{ m s}^{-1}$ . However, using the seasonal cycle to determine temporal

$\delta^{18}\text{O}$ -temperature relationship is fraught with many issues, the phenomena modeled here being only some of them [e.g., *Fisher et al.*, 1983; *Cuffey and Steig*, 1998; *Johnsen et al.*, 2000].

### 4.2. Spatial Variability Induced by Surface Topography

[61] Significant spatial variability has been found in  $\delta^{18}\text{O}$  of shallow cores from parts of the Antarctic Plateau with high accumulation rates [e.g., *Helsen et al.*, 2005]. Our model here inherently condenses two-dimensional effects into one-dimensional profiles. The source of the non-uniformity may be partially rooted in the dynamics of forced ventilation, which is assumed here to be a function of wind speed, but is also a function of sastrugi and dune behavior across the Antarctic Plateau. Besides wind speed, the amplitude of the pressure fluctuation across dunes or sastrugi is proportional to the height of the structure, and inversely proportional to its length (equation (4)). The snow structures parameterized here are 1-dimensional sinusoidal undulations; more realistic formulations for transverse and longitudinal undulations, i.e., more sastrugi-like parameterizations, are possible [*Cunningham and Waddington*, 1993]. Such parameterizations increase the amount of forced ventilation. However, with more peaks, there are more valleys, and the forced ventilation will vary on spatial scales related to sastrugi length and height scales. Given accumulation rates small enough to allow the influence of multiple years on any one layer of snow, the influence of dunes and sastrugi on  $\delta^{18}\text{O}$  may even out after a few years as they march along the snow surface.

[62] The behavior of dunes and sastrugi in Antarctica depends on many factors, including wind speed, temperature, surface snow grain size, solar radiation, and the

mechanical strength of the snow. A threshold wind speed is required to generate saltating and migrating snow grains [Mann *et al.*, 2000]. The magnitude of the threshold and the duration of winds necessary to induce snow migration depends on the history of the snow. High wind speeds at Dome C, for example, are likely less than at the South Pole [Wendler and Kodama, 1984], probably resulting in smaller sastrugi and dune structures. This would lead to less postdepositional modification of water stable isotopes by the mechanisms modeled here.

[63] Another influence significant to sastrugi morphology, and the results presented here, is solar radiation. The post-depositional modification due to the influence of the near-surface atmosphere in our model is greatest during the summers. During summer at the South Pole, sastrugi and dunes are flattened by differential heating of sastrugi faces by the spiraling Sun [Gow, 1965], whereas in our model, sastrugi exist with constant dimensions throughout the year. Solar flattening of sastrugi occurs to some degree across all of Antarctica, but is less diurnally uniform at lower latitudes. Dunes and sastrugi do form during summer under appropriate conditions; however, solar radiation and elevated summer temperatures lead to larger snow grain sizes, increasing the wind-speed threshold for snow migration and resulting in less frequent formation of dunes and sastrugi.

[64] The combination of the influences on sastrugi and dune dynamics therefore leads to larger sastrugi in the winter, and these sastrugi often last into late spring and early summer. The highest subsurface vapor pressures at the South Pole are during summer [Town *et al.*, 2008]. Fewer and smaller sastrugi during the summer, the time when forced ventilation of the snow can have the biggest effects, lead us to conclude that the optimal time for postdepositional modification is late spring when winter sastrugi still exist, but temperatures are high enough to affect the  $\delta^{18}\text{O}$  of winter snow. We use sastrugi dimensions typical of winter at the South Pole; by not including the seasonal effect of sastrugi height we probably exaggerate the effects of forced ventilation on  $\delta^{18}\text{O}$  of snow. However, sastrugi and dunes are still present during summer, and postdepositional modification of the snow  $\delta^{18}\text{O}$  can also happen without sastrugi.

#### 4.3. Last Glacial Maximum

[65] Post-depositional modification of water stable isotopes has important implications for the interpretation of reconstructions of glacial-interglacial temperature differences based on  $\delta^{18}\text{O}$  profiles from ice cores. Many of these reconstructions currently assume that the only influences on  $\delta^{18}\text{O}$  after deposition are molecular diffusion through pores in the firn, and much slower diffusion through the ice matrix after pore close-off [Johnsen *et al.*, 2000]. These effects result in a zero-bias smearing of annual signals, which is not important to reconstruction of glacial-interglacial temperature differences using  $\delta^{18}\text{O}$ . If atmospheric water vapor had an equal effect on the  $\delta^{18}\text{O}$  of near-surface snow in glacial and interglacial climates then there would also be no net effect on the  $\delta^{18}\text{O}$ -based reconstruction of glacial-interglacial temperature differences. However, in this section, we show that the magnitude of postdepositional modification between glacial and interglacial climates may differ significantly due only to differences in accumulation rate and temperature. We exclude changes in wind speed

and surface topography in the following simulations for lack of adequate knowledge of these parameters during glacial periods. However, faster wind speeds and rougher surfaces in glacial times would likely serve to make post-depositional modification even larger during glacial periods.

[66] As an example, we simulate the climate of Summit, Greenland during the present day and the Last Glacial Maximum (LGM). Figure 8 shows such a simulation, with the surface and subsurface temperature time series for present conditions at Summit, Greenland ( $T_{\text{ann}} \approx -27^\circ\text{C}$ ,  $\text{acc} \approx 25.2 \text{ cm a}^{-1}$  lwe, Cuffey and Clow [1997]), and during the LGM ( $T_{\text{ann}} \approx -47^\circ\text{C}$ ,  $\text{acc} \approx 6.3 \text{ cm a}^{-1}$  lwe, Cuffey and Clow [1997]). Of course, many climate factors affecting the final of the snow are expected to be different during the LGM (e.g.,  $\delta^{18}\text{O}$  of the evaporative source, atmospheric trajectories, wind speeds), but this example illustrates the combined influence of temperature and accumulation rate on isotopic modification of snow  $\delta^{18}\text{O}$  in a colder climate. In addition to Figure 8, the results are summarized in Table 1, which also includes a summary of results from all stable-isotope simulations.

[67] Again, a relatively high present-day accumulation rate inhibits significant postdepositional modification, while warmer temperatures encourage it. The lower accumulation rate during the LGM makes the  $\delta^{18}\text{O}$  record from Summit, Greenland more susceptible to enrichment by exposing each annual layer to more summertime atmospheric water vapor, even at temperatures of approximately  $-50^\circ\text{C}$ . The balance of these two competing influences, lower temperatures and lower accumulation rates, could result in a glacial-interglacial  $\delta^{18}\text{O}$  bias in either direction.

[68] The amount of late winter and spring enrichment in our present-day simulation of Summit, Greenland was large, 3.8‰ in the annual mean. In fact, with this set of conditions, the mean annual enrichment due to forced ventilation during the LGM is approximately equal to that of the present-day enrichment when the LGM accumulation rate is set to one-third of the present-day accumulation rate. A more realistic scenario (LGM accumulation rate = one-quarter present-day accumulation rate) yields greater enrichment during the LGM than the present day. The seasonality of the enrichment is significantly different between the two simulations; most of the present-day enrichment occurs during spring because of the high accumulation rate. This is moot as seasonal signals in  $\delta^{18}\text{O}$  are often not apparent in LGM ice. This difference in postdepositional modification will have a measurable affect on climate reconstructions using  $\delta^{18}\text{O}$ .

[69] The current reconstruction of the present-day-LGM temperature difference derived from borehole thermometry is 20 K, whereas it is 10 K when derived using the present-day  $\delta^{18}\text{O}$ -temperature relationship [Cuffey *et al.*, 1995]. Our results indicate that this discrepancy can be reduced by approximately 1.7 K by taking postdepositional modification into account. This correction to the discrepancy between borehole- and  $\delta^{18}\text{O}$ -derived temperature changes between present day and LGM is likely even larger because wind speeds and surface roughness are expected to be larger during the LGM. We did not include these factors in our LGM simulations because their current uncertainty is large.

[70] We performed the same experiment for Antarctic temperatures and accumulation rates, shown in Table 1

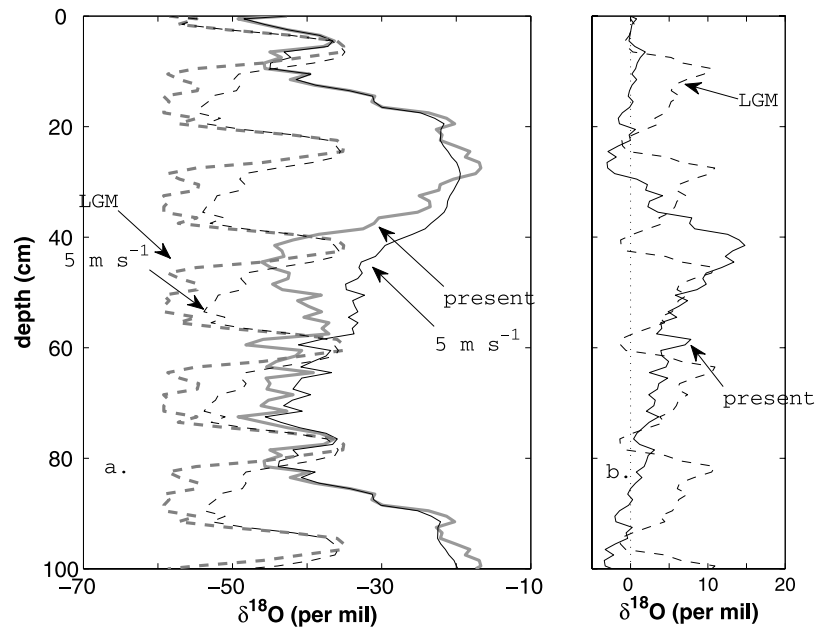


**Figure 8.** A simulation of the impact of LGM-like temperatures and accumulation rate on postdepositional enrichment in Greenland. (a) Solid lines depict  $\delta^{18}\text{O}$  as a result of approximate present-day temperature and accumulation rate at Summit, Greenland ( $T_{\text{ann}} = -27^\circ\text{C}$ ,  $\text{acc} = 25.2 \text{ cm a}^{-1}$  lwe), with and without postdepositional modification. The dashed lines depict when the temperature and accumulation rate are set to LGM levels ( $T_{\text{ann}} = -47^\circ\text{C}$ ,  $\text{acc} = 6.3 \text{ cm a}^{-1}$  lwe), with wind (black) and without wind (gray). (b) The solid lines are the residual between the present-day  $5 \text{ m s}^{-1}$  case and the present-day windless case. The dashed line is the residual between the LGM  $5 \text{ m s}^{-1}$  case and the LGM windless case.

[Lorius *et al.*, 1979, 1985; Petit *et al.*, 1999], where present-day Antarctic conditions are given in row 8 and LGM Antarctic conditions in row 7. In this case, it seems that the decrease in modification due to lower temperatures is almost exactly offset by the increase in modification due to a decrease in accumulation rate. Other interesting comparisons are the effect of accumulation on modification (compare rows 3–5, or rows 6 and 7), and the difference in enrichment due to the relationship of vapor pressure to temperature (compare rows 5 and 10, or rows 4 and 6).

#### 4.4. Improvement of the Model

[71] The model presented here has been constructed to illustrate the effect of atmospheric water vapor on  $\delta^{18}\text{O}$  of near-surface snow. While much effort has been made to keep the model quantitatively accurate, the model incorporates assumptions that have been made for conceptual and computational simplicity, and these assumptions may hinder quantitative interpretation. Improvement of the model parameterizations of accumulation rate, dune and sastrugi structure and evolution, and mass evolution in the model could improve the quantitative accuracy of the model as well as the adaptability of the model to site-specific climates.

[72] As stated earlier, simulating accumulation of snow as a continuous process (as is done here) is not strictly accurate anywhere; although it is arguably more appropriate on the high Antarctic Plateau than anywhere else in the world, because of diamond dust accumulation. In Antarctica, accumulation often comes episodically, especially along

the Antarctic coast, and therefore biases the isotopic record toward conditions associated with heavy precipitation [e.g., Schlosser *et al.*, 2004; Helsen *et al.*, 2005]. This model is currently capable of simulating variable accumulation rates, but seasonal and episodic accumulation rates for much of the Antarctic Plateau are not well-known, and are therefore difficult to simulate.

[73] Currently, the amount of snow isotopically averaged in the top volume is fixed to between 0.5 and 1.5 cm, and the vertical advection occurs in a sawtooth fashion. In reality, the depth of the top volume to be averaged depends on all the same variables that control sastrugi and dune formation and migration. Parameterizing the top-volume depth as a function of wind speed would increase the realism of the final isotopic mixture deposited on the snow surface prior to postdepositional modification by forced ventilation. Such parameterizations could also feed into the seasonal, or episodic, structure of sastrugi height and length, affecting the depth and seasonality of forced ventilation. More empirical information is required about these processes to improve the realism of mechanical mixing of snow in models.

[74] We have parameterized only the influence of surface water vapor on subsurface  $\delta^{18}\text{O}$ . However, pressure gradients across surface structures also cause pressure gradients within the snow, which most certainly causes vapor to be transported interstitially [Colbeck, 1989; Albert and McGilvary, 1992]. This vapor motion will have a further smoothing, but likely no biasing, effect on the seasonal cycle of  $\delta^{18}\text{O}$ . The smoothing will likely be largest during the

summer when vapor pressures are highest, despite the expected decrease in subsurface air-pressure gradients during summer due to sastrugi deflation.

[75] Sublimation during blowing-snow events, which can last for days, is also not parameterized here. During periods of high wind, snow can be lofted and widely redistributed. This process may also increase the mechanical mixing of snow, which would be parameterized as a change in the top level depth of the model. Blowing snow may lead to enhanced vapor transport in the atmosphere as the surface area of the snow grains increases because of fracture during saltation. Small grains are lofted high as warm air is transported downward, increasing vapor pressures, and potentially increasing postdepositional modification.

[76] Similarly, we have not allowed for the recycling of water vapor from the snowpack to the atmosphere and back to affect the  $\delta^{18}\text{O}$  of the near-surface snow. The degree to which this occurs on the Antarctic Plateau is uncertain. Our preliminary analyses indicate that synoptic influences have a 3–10 day frequency over the South Pole. We interpret this to mean that every 3–10 days the atmospheric scenario changes from a calm, clear scenario to a windy scenario with more coastal influence. Storms will bring in more moisture and energy, resetting the vapor content of the atmosphere from any vapor recycling that may have been previously occurring. These are the periods that are warmest, and when the most postdepositional modification likely occurs. Without more data on the degree of atmosphere-snowpack vapor reflux over the South Pole, it is difficult to construct an atmospheric scenario to drive our model in meaningful experiments on the effect of vapor reflux on  $\delta^{18}\text{O}$  of the near-surface snow.

[77] We have used a spatial  $\delta^{18}\text{O}$ -T relationship to specify  $\delta^{18}\text{O}$  of the falling snow. In some high-altitude Antarctic cases, the spatial  $\delta^{18}\text{O}$ -T relationship based on mean annual values of  $\delta^{18}\text{O}$  and temperature may be useful in a temporal sense because of the contribution of diamond dust to accumulation, and the deposition of near-surface atmospheric water vapor on diamond dust as it falls. Diamond dust is formed throughout the surface-based temperature inversion as evidenced by extreme clear-sky crystal habits found during the Antarctic winter [Walden *et al.*, 2003], crystal habits that often imply lower temperatures than observed at the inversion top [Bailey and Hallett, 2004]. So the diamond dust likely accumulates its  $\delta^{18}\text{O}$  signature throughout the temperature inversion, with a significant weighting to  $\delta^{18}\text{O}$  representing the inversion top due to the higher vapor pressures there. In any case, while a linear  $\delta^{18}\text{O}$ -T relationship may be accurate for some locations, and proves easier as a basis for understanding the effects of postdepositional modification of the  $\delta^{18}\text{O}$  of near-surface snow, a regional (or general) circulation model is likely a more accurate source of precipitation  $\delta^{18}\text{O}$  content to drive this model. This would eliminate uncertainty introduced by using equation (9) in such simulations, as well as unrealistic  $\delta^{18}\text{O}$  values introduced because of the temperature-dependent fractionation coefficient applied to equation (9).

## 5. Conclusions

[78] Post-depositional modification of the  $\delta^{18}\text{O}$  of near-surface snow remains a major uncertainty in polar paleo-

climate studies. We present here a preliminary attempt at understanding the different factors controlling vapor deposition and isotopic exchange in near-surface snow. Our results are based on a Rayleigh fractionation model in which pore-space diffusion, forced ventilation, and intra-ice-grain diffusion are parameterized by characteristic time constants that depend on atmospheric and glaciological conditions, such as atmospheric temperature, wind speed, snow temperature, snow grain size, snow density, sastrugi size and length, and accumulation rate.

[79] With this model it is possible to simulate a specific ice core, given all the atmospheric and glaciological conditions. We have primarily simulated ice cores at the South Pole, using them as a basis for evaluating the sensitivity of the model parameterizations to different boundary conditions. Some specific results are summarized in Table 1. In general, we find enrichment of  $^{18}\text{O}$  in winter snow layers, which occurs during subsequent summers. Low-accumulation-rate sites experience sizable winter enrichment because the winter snow is exposed to several summers of forced ventilation. Given an appropriate accumulation rate, there is a slight depletion of  $^{18}\text{O}$  in summer snow.

[80] We find that forced ventilation is more important than pore-space diffusion to postdepositional modification because of the different range of influence of the two processes. Pore-space diffusion is significant on annual time scales only in the top one to two centimeters of snow, and is therefore not often acting on snow that differs significantly in  $\delta^{18}\text{O}$  from recent accumulation. Pore-space diffusion may become more important in cases of extremely low accumulation rates coupled with low wind speeds; i.e., over domes.

[81] Forced ventilation of the snow and snow vapor pressure are both nonlinear phenomena with respect to wind speed and temperature, respectively. One might expect that simulations using daily wind speeds with daily temperatures would enrich the snow more than using a constant (mean annual) wind speed for the whole year. However, variable-wind-speed simulations show similar enrichments as constant-wind-speed simulations when other factors are equal because of the partially compensating effects of summertime enrichment and wintertime depletion.

[82] On glacial time scales, all factors being equal but temperature, we find that postdepositional modification exaggerates the difference between inferred glacial and interglacial temperatures. In simulating Summit, Greenland during the present day and the LGM using different accumulation rates and temperatures, we find that higher present-day temperatures coupled with higher accumulation rates will induce a large spring and late-winter enrichment of  $\delta^{18}\text{O}$ , and that mean LGM temperatures and accumulation rates at Summit, Greenland allow significant postdepositional modification. In this case, the enrichment of  $^{18}\text{O}$  during the LGM is greater than during the present day, slightly increasing the  $\delta^{18}\text{O}$ -based reconstructed temperature difference between the present and the LGM. We have assumed that wind speeds and sastrugi are the same in both glacial and interglacial times; relaxation of these assumptions would likely act to increase postdepositional modification during the LGM. In the current simulations, the  $^{18}\text{O}$  enrichment during the LGM in Antarctica is approximately equal to that of the present day because of the compensating factors of decreased accumulation and decreased temperatures.

[83] The results presented here are based on established parameterizations of the atmosphere and of snow. However, there is much room to refine their implementation and, more importantly, a comparison to observations is necessary.

[84] **Acknowledgments.** We thank Howard Conway, Tom Neumann, Eric Steig, and Hans Christian Steen-Larsen for helpful discussions on water stable isotopes. Elisabeth Schlosser and two anonymous reviewers provided useful comments and suggestions. Eells Dutton and Tom Mefford of NOAA ESRL-GMD provided us with the South Pole data set used in simulations. This work was funded under National Science Foundation grants OPP-0540090 and OPP-0636997.

## References

- Albert, M. R., and W. R. McGilvary (1992), Thermal effects due to air flow and vapor transport in dry snow, *J. Glaciol.*, *38*, 273–281.
- Aldaz, L., and S. Deutsch (1967), On a relationship between air temperature and oxygen isotope ratio of snow and firn in the South Pole region, *Earth Planet. Sci. Lett.*, *3*, 2667–2674.
- Bailey, M., and J. Hallett (2004), Growth rates and habits of ice crystals between  $-20^{\circ}\text{C}$  and  $-70^{\circ}\text{C}$ , *J. Atmos. Sci.*, *61*, 514–544.
- Brandt, R. E., and S. G. Warren (1997), Temperature measurements and heat transfer in the near-surface snow at the South Pole, *J. Glaciol.*, *43*, 339–351.
- Bromwich, D. H., and T. R. Parish (1998), Meteorology of the Antarctic, in *Meteorological Monographs: Meteorology of the Southern Hemisphere*, vol. 27, edited by D. J. Karoly and D. G. Vincent, pp. 175–200, Am. Meteorol. Soc., Boston, Mass.
- Ciais, P., and J. Jouzel (1994), Deuterium and oxygen 18 in precipitation: Isotopic model, including mixed-cloud processes, *J. Geophys. Res.*, *99*(D8), 16,793–16,803.
- Colbeck, S. C. (1989), Air movement in snow due to wind-pumping, *J. Glaciol.*, *35*, 209–213.
- Cuffey, K. M., and G. D. Clow (1997), Temperature, accumulation, and ice sheet elevation in central Greenland through the last deglacial transition, *J. Geophys. Res.*, *102*, 26,383–26,396.
- Cuffey, K. M., and E. J. Steig (1998), Isotopic diffusion in polar firn: Implications for interpretation of seasonal climate parameters in ice-core records, with emphasis on central Greenland, *J. Glaciol.*, *44*(174), 273–284.
- Cuffey, K. M., G. D. Clow, R. B. Alley, M. Stuiver, E. D. Waddington, and R. W. Saltus (1995), Large arctic temperature change at the Wisconsin-Holocene glacial transition, *Science*, *270*, 455–458.
- Cunningham, J., and E. D. Waddington (1993), Air flow and dry deposition of non-sea salt sulfate in polar firn: Paleoclimate implications, *Atmos. Environ.*, *27A*(17–18), 2943–2956.
- Dansgaard, W. (1964), Stable isotopes in precipitation, *Tellus*, *16*, 436–468.
- Dansgaard, W., S. J. Johnsen, H. B. Clausen, and N. Gundestrup (1973), Stable isotope glaciology, *Medd. Grøn.*, *197*(2), 1–53.
- Ekaykin, A. A., V. Y. Lipenkov, N. I. Barkov, J. R. Petit, and V. Masson-Delmotte (2002), Spatial and temporal variability in isotope composition of recent snow in the vicinity of Vostok Station, Antarctica: Implications for ice-core record interpretation, *Ann. Glaciol.*, *35*, 181–186.
- Ekaykin, A. A., V. Y. Lipenkov, I. N. Kuzmina, J. R. Petit, V. Masson-Delmotte, and S. J. Johnsen (2004), The changes in isotope composition and accumulation of snow at Vostok station, East Antarctica, over the past 200 years, *Ann. Glaciol.*, *39*, 569–575.
- EPICA Members (2004), Eight glacial cycles from an Antarctic ice core, *Nature*, *429*(6992), 623–628.
- Epstein, S., R. P. Sharp, and A. J. Gow (1965), Six-year record of oxygen and hydrogen isotope variations in South Pole firn, *J. Geophys. Res.*, *70*, 1809–1814.
- Fisher, D. A., R. M. Koerner, W. S. B. Paterson, W. Dansgaard, N. Gundestrup, and N. Reeh (1983), Effect of wind scouring on climatic records from ice-core oxygen-isotope profiles, *Nature*, *301*, 205–209.
- Friedman, I., C. Benson, and J. Gleason (1991), Isotopic changes during snow metamorphism, in *Stable Isotope Geochemistry: A Tribute to Samuel Epstein*, edited by J. R. O'Neill and I. R. Kaplan, pp. 211–221, Geochem. Soc., Washington, D. C.
- Fujita, K., and O. Abe (2006), Stable isotopes in daily precipitation at Dome Fuji, East Antarctica, *Geophys. Res. Lett.*, *33*, L18503, doi:10.1029/2006GL026936.
- Gow, A. J. (1965), On the accumulation and seasonal stratification of snow at the South Pole, *J. Glaciol.*, *5*, 467–477.
- Grenfell, T. C., S. G. Warren, and P. C. Mullen (1994), Reflection of solar radiation by the Antarctic snow surface at ultraviolet, visible, and near-infrared wavelengths, *J. Geophys. Res.*, *99*(D9), 18,669–18,684.
- Grootes, P. M., E. Steig, and M. Stuiver (1994), Taylor Ice Dome study 1993–1994: An ice core to bedrock, *Antarct. J. U.S.*, *29*(5), 79–81.
- Helsen, M. M., R. S. W. van de Wal, M. R. van den Broeke, D. van As, H. A. J. Meijer, and C. H. Reijmer (2005), Oxygen isotope variability in snow from western Dronning Maud Land, Antarctica and its relation to temperature, *Tellus*, *57*(5), 423–435.
- Helsen, M. M., R. S. W. van de Wal, M. R. van den Broeke, V. Masson-Delmotte, H. A. J. Meijer, M. P. Scheele, and M. Werner (2006), Modeling the isotopic composition of Antarctic snow using backward trajectories: Simulation of snow pit records, *J. Geophys. Res.*, *111*, D15109, doi:10.1029/2005JD006524.
- Helsen, M. M., R. S. W. van de Wal, and M. R. van den Broeke (2007), The isotopic composition of present-day Antarctic snow in a Lagrangian simulation, *J. Clim.*, *20*, 739–756.
- Hogan, A. W. (1975), Summer ice crystal precipitation at the South Pole, *J. Appl. Meteorol.*, *14*, 246–249.
- Jakli, G., and D. Staschewski (1977), Vapor pressure of  $\text{H}_2^{18}\text{O}$  ice ( $-50$  to  $0^{\circ}\text{C}$ ) and  $\text{H}_2^{18}\text{O}$  water ( $0$  to  $170^{\circ}\text{C}$ ), *J. Chemical Soc., Faraday Trans. 1*, *73*(10), 1505–1509.
- Jansco, G., J. Pupezin, and W. A. V. Hook (1970), Vapour pressure of  $\text{H}_2^{18}\text{O}$  ice (I) ( $-17^{\circ}\text{C}$  to  $0^{\circ}\text{C}$ ) and  $\text{H}_2^{18}\text{O}$  water ( $0^{\circ}\text{C}$  to  $-16^{\circ}\text{C}$ ), *Nature*, *225*, 723.
- Johnsen, S. J. (1977), Stable isotope homogenization of polar firn and ice, in *Isotopes and Impurities in Snow and Ice*, Proceedings of the Grenoble Symposium, August/September 1975, pp. 210–219, IAHS AISH Publ., 118, Grenoble, France.
- Johnsen, S. J., H. B. Clausen, K. M. Cuffey, G. Hoffman, J. Schwander, and T. Creyts (2000), Diffusion of stable isotopes in polar firn and ice: The isotope effect in firn diffusion, in *Physics of Ice Core Records*, edited by T. Hondoh, pp. 121–140, Hokkaido Univ. Press, Sapporo, Japan.
- Johnsen, S. J., D. Dahl-Jensen, N. Gundestrup, J. P. Steffensen, H. B. Clausen, H. Miller, V. Masson-Delmotte, A. E. Sveinbjörnsdóttir, and J. White (2001), Oxygen isotope and palaeotemperature records from six Greenland ice-core stations: Camp Century, DYE-3, GRIP, GISP2, Renland and NorthGRIP, *Quat. Res.*, *16*(4), 299–307.
- Jouzel, J., and L. Merlivat (1984), Deuterium and oxygen 18 in precipitation: Modeling of the isotopic effects during snow formation, *J. Geophys. Res.*, *89*, 11,749–11,757.
- Jouzel, J., L. Merlivat, J. R. Petit, and C. Lorius (1983), Climatic information over the last century deduced from a detailed isotopic record in the South Pole snow, *J. Geophys. Res.*, *88*, 2693–2703.
- Jouzel, J., et al. (1997), Validity of the temperature reconstruction from water isotopes in ice cores, *J. Geophys. Res.*, *102*, 26,471–26,487.
- Jouzel, J., F. Vimeux, N. Caillon, G. Delaygue, G. Hoffman, V. Masson-Delmotte, and F. Parrenin (2003), Magnitude of isotope/temperature scaling for interpretation of central Antarctic ice cores, *J. Geophys. Res.*, *108*(D12), 4361, doi:10.1029/2002JD002677.
- Krinner, G., and M. Werner (2003), Impact of precipitation seasonality changes on isotopic signals in polar ice cores: A multi-model analysis, *Earth Planet. Sci. Lett.*, *216*, 525–538.
- Kuhn, M., A. J. Riordan, and I. A. Wagner (1975), The climate of Plateau Station, in *Climate of the Arctic*, edited by G. Weller and S. A. Bowling, pp. 255–267, Am. Meteor. Soc., Boston, Mass.
- Lorius, C., L. Merlivat, J. Jouzel, and M. Pourchet (1979), A 30,000-yr isotope climatic record from Antarctic ice, *Nature*, *280*(5724), 644–648.
- Lorius, C., J. Jouzel, C. Ritz, L. Merlivat, N. I. Barkov, Y. S. Korotkevich, and V. M. Kotlyakov (1985), A 150,000-yr climatic record from Antarctic ice, *Nature*, *316*(6029), 591–596.
- Majoube, M. (1970), Fractionation factor of  $^{18}\text{O}$  between water vapour and ice, *Nature*, *226*, 1242.
- Mann, G. W., P. S. Anderson, and S. D. Mobbs (2000), Profile measurements of blowing snow at Halley, Antarctica, *J. Geophys. Res.*, *105*, 24,491–24,508.
- Matsuo, S., and O. Matsubaya (1969), Vapor pressure of  $\text{H}_2^{18}\text{O}$  ice, *Nature*, *221*, 463–464.
- Mayewski, P. A., et al. (2005), The International Trans-Antarctic Scientific Expedition (ITASE): An overview, *Ann. Glaciol.*, *41*, 180–185.
- Mosley-Thompson, E., J. F. Paskievitch, A. J. Gow, and L. G. Thompson (1999), Late 20th century increase in South Pole accumulation, *J. Geophys. Res.*, *104*, 3877–3886.
- Neumann, T. A., and E. D. Waddington (2004), Effects of firn ventilation on isotopic exchange, *J. Glaciol.*, *169*(50), 183–194.
- Neumann, T. A., E. D. Waddington, E. J. Steig, and P. M. Grootes (2005), Non-climate influences on stable isotopes at Taylor Mouth, Antarctica, *J. Glaciol.*, *173*, 248–258.
- Neumann, T. A., M. R. Albert, R. Lomonaco, C. Engel, Z. Courville, and F. Perron (2008), Experimental determination of snow sublimation rate and stable-isotopic exchange, *Ann. Glaciol.*, *49*, 1–6.
- Petit, J. R., et al. (1999), Climate and atmospheric history of the past 420,000 years from the Vostok ice core, Antarctica, *Nature*, *399*, 429–436.

- Schlosser, E., C. Reijmer, H. Oerter, and W. Graf (2004), The influence of precipitation origin on the  $\delta^{18}\text{O}$ -T relationship at Neumayer station, Ekströmisen, Antarctica, *Ann. Glaciol.*, *39*, 41–48.
- Schwerdtfeger, W. (1970), The climate of the Antarctic, in *World Survey of Climatology*, vol. 14, edited by E. Landsberg, pp. 253–355, Elsevier, Amsterdam, Netherlands.
- Steig, E., et al. (2005), High-resolution ice cores from US ITASE (West Antarctica): Development and validation of chronologies and determination of precision and accuracy, *Ann. Glaciol.*, *41*, 77–84.
- Stichler, W., U. Schotterer, K. Fröhlich, P. Ginot, C. Kull, H. Gäggeler, and B. Pouyaud (2001), Influence of sublimation on stable isotope records recovered from high-altitude glaciers in the tropical Andes, *J. Geophys. Res.*, *106*, 22,613–22,620.
- Town, M. S., V. P. Walden, and S. G. Warren (2005), Spectral and broadband longwave downwelling radiative fluxes, cloud radiative forcing and fractional cloud cover over the South Pole, *J. Clim.*, *18*(20), 4235–4252.
- Town, M. S., E. D. Waddington, V. P. Walden, and S. G. Warren (2008), Subsurface temperatures, heating rates, and vapor pressures in the near-surface snow of East Antarctica, *J. Glaciol.*, *54*(186), 487–498.
- Waddington, E. D., J. Cunningham, and S. L. Harder (1996), The effects of snow ventilation on chemical concentrations, in *Chemical Exchange Between the Atmosphere and Polar Snow (NATO ASI Series I: Global Environmental Change 43)*, edited by E. W. Wolff and R. C. Bales, pp. 403–451, Springer-Verlag, Berlin, Germany.
- Waddington, E. D., E. J. Steig, and T. A. Neumann (2002), Using characteristic times to assess whether stable isotopes in polar snow can be reversibly deposited, *Ann. Glaciol.*, *35*, 118–124.
- Walden, V. P., S. G. Warren, and E. Tuttle (2003), Atmospheric ice crystals over the Antarctic Plateau in winter, *J. Clim.*, *42*, 1391–1405.
- Wendler, G., and Y. Kodama (1984), On the climate of Dome C, Antarctica, in relation to its geographical setting, *Int. J. Climatol.*, *4*(5), 495–508.
- Whillans, I. M., and P. M. Grootes (1985), Isotopic diffusion in cold snow and firn, *J. Geophys. Res.*, *90*, 3910–3918.
- 
- M. S. Town and S. G. Warren, Department of Atmospheric Sciences, University of Washington, Box 351640, Seattle, WA 98195-1640, USA. (mstown@atmos.washington.edu)
- E. D. Waddington, Department of Earth and Space Sciences, University of Washington, Johnson Hall 070, Box 351310, 400 15th Avenue NE, Seattle, WA 98195-1310, USA.
- V. P. Walden, Department of Geography, University of Idaho, McClure Hall, Room 305B, Moscow, ID 83844-3021, USA.